Title:

Heme's relevance genuine? Re-visiting the roles of TANGO2 homologs including HRG-9 and HRG-10 in *C. elegans*

Authors:

Sandkuhler, Sarah E.,[1] Youngs, Kayla S.,[2] Gottipalli, O.,[3] Owlett, Laura,[2] Bandora, Monica B.,[4] Naaz, Aaliya,[5] Kim, Euri S.,[6] Wang, Lili,[7] Wojtovich, Andrew P.,[8] Gupta, Vandana A.,[6] Sacher, Michael,[5,9] Mackenzie, Samuel, J.[2]

Affiliations:

1 - Department of Pathology, University of Rochester Medical Center, Rochester, NY

2 - Department of Neurology, University of Rochester Medical Center, Rochester, NY

3 - Emory University, Atlanta, GA

4 - Morgan State University, Baltimore, MD

5 - Department of Biology, Concordia University, Montreal, Canada

6 - Department of Medicine, Brigham and Women's Hospital Harvard Medical School, Boston, MA

7 - Department of Pharmacology, Vanderbilt University, Nashville, TN

8 - Department of Anesthesiology and Perioperative Medicine, University of Rochester Medical Center, Rochester, NY

9 - Department of Anatomy and Cell Biology, McGill University, Montreal, Canada

Corresponding Author:

Samuel J. Mackenzie

University of Rochester Medical Center

Room 1-9644 KMRB

601 Elmwood Ave

Rochester, NY 14642

Samuel_mackenzie@urmc.rochester.edu

585-276-6503

Abstract:

Mutations in the *TANGO2* gene are associated with a severe neurometabolic disorder in humans, often presenting with life-threatening metabolic crisis. However, the function of TANGO2 protein remains unknown. It has recently been proposed that TANGO2 transports heme within and between cells, from areas with high heme concentrations to those with lower concentrations. Here, we demonstrate that prior heme-related observations in *Caenorhabditis elegans* lacking TANGO2 homologs HRG-9 and HRG-10 may be better explained by a previously unreported metabolic phenotype, characterized by reduced feeding, decreased lifespan and brood sizes, and poor motility. We also show that several genes not implicated in heme transport are upregulated in the low heme state and conversely demonstrate that *hrg-9* in particular is highly responsive to oxidative stress, independent of heme status. Collectively, these data implicate bioenergetic failure and oxidative stress as potential factors in the pathophysiology of TANGO2 deficiency, in alignment with observations from human patients. Our group performed several experiments in yeast and zebrafish deficient in TANGO2 homologs and was unable to replicate prior findings from these models. Overall, we believe there is insufficient evidence to support heme transport as the primary function for TANGO2.

Impact statement:

Cross-species examination of TANGO2 homologs demonstrates that phenotypes previously attributed to altered heme trafficking may instead reflect broader disturbances in mitochondrial function and cellular homeostasis.

Introduction:

Transport and Golgi Organization 2 (TANGO2) Deficiency Disorder (TDD) is a severe, progressive, neurodegenerative disease primarily affecting children and young adults, frequently accompanied by recurrent, life-threatening metabolic crises.[1-4] While TANGO2 is conserved in species across all three domains of life, its cellular function has not been fully elucidated. Initially identified in a screen of *Drosophila* genes which, when depleted, precipitate ER-Golgi fusion defects,[5] TANGO2 has since been shown to localize to both the cytoplasm and the mitochondria.[6,7] Mutations in TANGO2 have been associated with altered mitochondrial respiration and morphology,[8] disregulated lipid homeostasis[9,10] and defects in fatty acid oxidation[8] in multiple models. Treatment with supplemental pantothenic acid, the precursor of coenzyme A (CoA), has been shown to improve lipid profile abnormalities in cells,[10] rescue phenotypic defects in a *Drosophila* TDD model,[11] and potentially reduce metabolic crises in patients,[12] implicating reduced CoA, lipid dysregulation, and impaired mitochondrial function as putative drivers of TDD symptoms.

A recent study by Sun et al. suggested that two *Caenorhabditis elegans* homologs of TANGO2, HRG-9 and HRG-10 (Heme-Responsive Gene), play a critical role in heme export from intestinal cells and lysosome-related organelles and that TANGO2 exhibits a similar function in mobilizing heme from mitochondria in other eukaryotic organisms including yeast.[13] Two subsequent studies also reported that TANGO2 is involved in heme transport, albeit via discordant mechanisms.[14,15] The notion that defective heme transport underlies the pathophysiology of TANGO2 deficiency marks a sizeable shift from the emerging scientific consensus that TANGO2 is critical for CoA and lipid homeostasis. Therefore, our primary objective was to validate key findings pertaining to heme transport in *C. elegans* while also replicating key findings in zebrafish and yeast lacking TANGO2 homologs. We hypothesized that, if present, defects in heme transport may be downstream features of aberrant cellular metabolism and thus may not be central to the pathophysiology of TDD.

Results:

C. elegans lacking TANGO2 homologs (double knockout; DKO) demonstrate modest survival benefit upon toxic heme analog exposure

We first sought to validate results from prior experiments using heme analogs in worms lacking both HRG-9 and HRG-10 (double knockout; DKO). In previous studies, DKO worms exposed to 1 µM concentration of the toxic heme analog gallium protoporphyrin IX (GaPP) showed a significant survival benefit in contrast with nearly uniform lethality in wild type (Bristol N2) worms.[13] We exposed gravid DKO and N2 nematodes to GaPP at varying concentrations, removing P_0 worms at 24 hours, and counting alive and dead F_1 progeny at 72 hours. While we required relatively higher concentrations of GaPP to achieve lethality, all strains exhibited a clear dose-dependent reduction in survival (Figure 1A). A statistically significant group effect was observed at 2 µM, with DKO worms showing a modest relative survival benefit compared to N2.

DKO *C. elegans* demonstrate increased lawn avoidance and reduced pharyngeal pumping

In maintaining the DKO strain under basal conditions (i.e., no GaPP exposure), we incidentally observed relatively intact *E. coli* lawns on plates housing DKO worms compared to N2 plates. On closer examination, DKO worms demonstrated several previously undescribed phenotypic features including lawn avoidance, a greater propensity for crawling off plates, reduced pharyngeal pumping, and decreased survival (Figure 2A, B, and F). Based on these observations, we hypothesized that the GaPP survival difference in our initial experiment might have been driven, at least in part, by reduced GaPP consumption. We therefore also examined the effect of GaPP exposure on worms lacking a pharyngeal acetylcholine receptor subunit (*eat-2*(*ad465*)). The *eat-2* strain exhibits reduced pharyngeal pumping and has been used extensively as a model of dietary restriction.[16,17] Of the three strains tested, survival was highest in *eat-2* mutants (Figure 1A) despite the fact that these worms have no known defects in heme metabolism or transport.

DKO *C. elegans* demonstrate reduced ZnMP fluorescence

DKO nematodes at the L4 larval stage were previously shown to accumulate the fluorescent heme analog zinc mesoporphyrin IX (ZnMP) in intestinal cells in low-heme (4 µM) liquid media. While attempting to replicate this experiment, we observed that both wildtype and DKO nematodes entered L1 arrest under these conditions. Therefore, to allow for developmental progression, we grew worms on standard OP50 *E. coli* plates and in media containing physiological levels of heme (20 µM). We then examined whether differences in ZnMP uptake persisted under these basal conditions. DKO worms grown on ZnMP-treated *E. coli* plates displayed significantly reduced intestinal ZnMP fluorescence compared to N2 (Figure 1B and C). Using basal heme media with ZnMP, there was no significant difference in ZnMP fluorescence between DKO and wildtype nematodes, although DKO worms grown in media without ZnMP exhibited significantly higher autofluorescence (Figure 1D and E). To test whether autofluorescence may have contributed to the higher fluorescent intensities previously reported in heme-deficient DKO worms, we repeated this experiment on agar plates under starved conditions but did not observe a difference between groups (Figure 1B).

DKO *C. elegans* demonstrate multiple features suggestive of bioenergetic dysfunction

In assessing brood survival in the GaPP assay, we also observed significantly smaller starting broods for DKO nematodes, a previously unreported finding that persisted in the absence of GaPP (Figure 2C). As oogenesis and egg-laying require a high energetic expenditure for gravid *C. elegans*, reduced brood size is a known feature of several metabolically impaired nematode strains.[18,19] We also observed reduced movement on the plate from DKO worms and decided to further characterize the worms' capacity for movement by subjecting them to a swim exhaustion assay. Nematodes were placed in isotonic M9 buffer and scored on their swimming ability at 4 minute intervals. While *C. elegans* are typically able to swim continuously for up to 90 minutes in M9 media,[20] we observed that the DKO worms quickly became exhausted and could not maintain normal swimming shortly after being placed in media

(Figure 2D). We further quantified the rate of thrashing in M9 media during the first 4-minute interval and found that DKO worms thrashed 61% slower compared to N2 (Figure 2E).

Oxidative stress is a driver of TANGO2 homolog transcription

Given previous observations implicating oxidative stress as a hallmark feature of TDD,[8] we next sought to examine what other genes were enriched under low heme conditions. We reanalyzed the RNA-seq dataset generated by Sun et al., employing the Empirical Analysis of Gene Expression in R (edgeR) package on raw counts to accurately perform between-group comparisons across low (2 µM), optimal (20 µM), and high (400 µM) heme conditions. We extracted the top 500 enriched genes and plotted those that showed significantly increased expression in the low heme state, based on computational clustering (N=134; Figure 3A). Several genes with no known heme-related functions demonstrated stronger relative expression and higher likelihood ratios of conditional effect than did *hrg-9*. Furthermore, gene ontology analysis of genes with similar enrichment to *hrg-9* revealed a wide spectrum of biological processes and cellular roles, including but not limited to collagen deposition, cellular detoxification, and lipid binding (Figure 3B). To test what alternate forms of cell stress might induce *hrg-9* and *hrg-10* expression, we exposed N2 nematodes to heat (34°C), starvation (24 hours without OP50), and paraquat (25 mM), a potent generator of superoxide, with subsequent measurement of transcriptional enrichment by way of RT-qPCR. We observed a 12-fold enrichment of *hrg-9* after paraquat exposure, suggesting that its expression may be linked to oxidative stress more broadly and is not uniquely driven by heme levels (Figure 3C).

Yeast deficient in TANGO2 homolog YGR127w exhibit normal growth

As Sun et al. also examined the function of TANGO2 homologs in yeast (YGR127w) and zebrafish (tango2), we sought to validate their findings in these models. It was previously reported that the *ygr127w* yeast knockout exhibits a severe temperature sensitive growth defect and impaired heme distribution. We also observed a growth defect in the strain generated by Sun et al.; however, two separate strains on different backgrounds (BY4741 and BY4742) and a

third strain generated by our lab (W303-1a) showed normal growth (Figure 4A). The growth defect in the initial yeast strain reported by Sun et al. was also not rescued with YGR127w complementation. As the background for this strain is known to be prone to mitochondrial genome instability,[21] we hypothesize that this line may harbor a secondary mutation.

Myofiber defects in tango2-deficient zebrafish

In zebrafish, Sun et al. reported no discernable phenotype in *tango2*$^{-/-}$ fish bred from heterozygous parents but observed severe skeletal muscle damage in *tango2*$^{-/-}$ larvae from *tango2*$^{-/-}$ parents. In a recent study, we showed increased lethality and reduced phospholipid and triglyceride levels in *tango2*$^{-/-}$ fish obtained from heterozygous parents.[22] *tango2*$^{-/-}$ larvae from two different alleles (tango2^{bwh210} and tango2^{bwh211}) exhibited defects in myofiber organization irrespective of heterozygous or homozygous parents (Figure 4B) but lacked the striking muscle damage previously reported.

Discussion:

Our data, coupled with clinical observations in TDD, do not support a primary role for TANGO2 as a heme chaperone. In *C. elegans* lacking TANGO2 homologs, we were unable to fully replicate prior findings of defective heme transport using toxic and fluorescent heme analogs. Parallel studies in yeast and zebrafish failed to reproduce previously reported phenotypes in growth and muscle fiber integrity, respectively.

Exposing worms to GaPP, a toxic heme analog, we observed that nematodes deficient in HRG-9 and HRG-10 displayed increased survival compared to WT worms, consistent with prior work,[13] though the between-group difference was markedly smaller in our study. We required higher GaPP concentrations to induce lethality, potentially due to product vendor differences, but did observe a clear dose-dependent effect across strains. Although it was previously proposed that the survival benefit seen in worms lacking HRG-9 and HRG-10 resulted from reduced transfer from intestinal cells after GaPP ingestion, our data suggest the

reduced lethality is more likely due to decreased environmental GaPP uptake. Supporting this notion, DKO worms exhibited lawn avoidance, reduced pharyngeal pumping, and modestly lower intestinal ZnMP accumulation when exposed to this fluorescent heme analog on agar plates. In liquid media, DKO worms demonstrated higher fluorescence, but only in ZnMP-free conditions, suggesting the presence of gut granule autofluorescence. Furthermore, survival following exposure to GaPP was highest in *eat-2* mutants, despite heme trafficking being unaffected in this strain.

In addition to altered pharyngeal pumping, DKO worms displayed multiple previously unreported phenotypic features, suggesting a broader metabolic impairment and reminiscent of some clinical manifestations observed in patients with TDD. Elucidating the mechanisms underlying this phenotype, and whether they reflect a core bioenergetic defect, is an active area of investigation in our lab. Several *C. elegans* heme-responsive genes have been characterized, revealing relatively specific defects in heme uptake or utilization rather than broad organismal dysfunction. For example, *hrg-1* and *hrg-4* mutants exhibit impaired growth only under heme-limited conditions,[23] and *hrg-3* loss affects brood size and embryonic viability specifically when maternal heme is scarce.[24] By contrast, *hrg-9* and *hrg-10* mutants exhibit the most severe phenotypes of the hrg family, to date, including reduced pharyngeal pumping, decreased motility, shortened lifespan, and smaller broods, even when fed a heme-replete diet.

Laboratory abnormalities in human patients TDD include abnormal acylcarnitine profiles, hyperammonemia, and elevated creatinine kinase levels during metabolic crises,[3,12] while abnormalities associated with defective heme transport (e.g., erythrocyte membrane defects, low hemoglobin levels) have not been observed in patients with this condition. Strikingly, retrospective data suggest that patients with TDD receiving B-vitamin supplementation inclusive of pantothenic acid, a precursor of CoA, do not experience metabolic crises[12] and show substantial improvement in other domains as well. Pantothenic acid supplementation also

yielded full phenotypic rescue in a *Drosophila* model of TDD.[11] It is difficult to reconcile how this treatment would be beneficial in a condition characterized by dysregulated heme trafficking.

Heme is a hydrophobic molecule; thus, it is plausible that if TANGO2 and its homologs are involved in lipid binding, as was recently demonstrated in Hep2G cells,[7] these proteins may also weakly bind heme.[14] Han et al. demonstrated that a bacterial heme homolog, HtpA, directly binds heme and is necessary for cytochrome c function.[14] We would note, however, that TANGO2 was not among the 378 heme-binding proteins identified on a recent proteomic screen of three separate cell lines.[25] Jayaram et al. recently proposed that TANGO2 may instead interact with the mitochondrial heme exporter FLVCR1b to release mitochondrial heme without directly binding to heme itself, though this interaction was observed only after heme synthesis was potentiated via d-ALA and iron supplementation, raising questions about the role of TANGO2 under basal heme conditions.[15] Furthermore, the investigators identified GAPDH as the exclusive binding partner of heme upon export through FLVCR1b. How GAPDH, a protein important for multiple cellular functions, including glycolysis, is affected in TDD remains unknown.

In this study, we demonstrated that *hrg-9* expression is strongly induced by paraquat, a generator of superoxide free radical. Prior work has also identified *hrg-9* as a major transcriptional target of the mitochondrial unfolded protein response (mtUPR) through ATFS-1 transcription factor binding.[26,27] Given that heme is an essential component of cytochromes in the electron transport chain, heme deficiency could plausibly activate *hrg-9* through the induction of mitochrondial stress. Conversely, artificially stimulating heme synthesis may exert a similar transcriptional effect, as excess heme is mitotoxic and can itself trigger a stress response. Indeed, *hrg-9* was also shown to be modestly up-regulated in the high-heme state, unlike other genes in the *hrg* family (Figure 3A), and our reanalysis of an RNA-seq dataset examining transcription under low-heme conditions revealed broad induction of stress-responsive genes with no established role in heme trafficking (Figure 3B).

In summary, our findings challenge the notion that TANGO2 functions as a heme chaperone. Instead, and consistent with growing clinical evidence, they support a model in which TANGO2 may help mitigate cellular stress and maintain mitochondrial function under conditions of redox imbalance (Figure 5). Clearly, further work is needed to define the precise role of this highly conserved protein as we work to develop effective treatments for patients with TDD.

Materials and methods:

Key Resources Table				
Reagent type (species) or resource	**Designation**	**Source or reference**	**Identifiers**	**Additional information**
strain (Caenorhabditis elegans)	N2	Caenorhabditis Genetics Center (CGC) at the University of Minnesota	Bristol N2	
strain (Caenorhabditis elegans)	Double knockout (DKO)	Chen Lab, Zhejiang University	CCH303 (hrg-9(cck301)V; hrg-10(cck302)V)	Sun et al., 2022
strain (Caenorhabditis elegans)	eat-2	Samuelson Lab, University of Rochester	eat-2(ad465)	Raizen & Avery, 1995
chemical compound, reagent	gallium protoporphyrin IX chloride (GaPP)	Santa Cruz	CAS 210409-12-4	GaPP used in Sun et al., 2022 souced from Frontier Scientific
chemical	Zn(II)	Santa	CAS 14354-67-	ZnMP used in Sun et al., 2022

compound, reagent	Mesoporphyrin IX (ZnMP)	Cruz	7	souced from Frontier Scientific
software, algorithm	Empirical Analysis of Gene Expression in R (edgeR)	Bioconductor.org		Chen et al., 2025
software, algorithm	WormCat	Github.com		Holdorf et al., 2020
chemical compound, reagent	Paraquat (methyl viologen dichloride hydrate)	Sigma Aldrich	856177	
chemical compound, reagent	TRIzol	Invitrogen	15596026	
commercial assay or kit	RNeasy Mini Kit	Qiagen	74104	
commercial assay or kit	Maxima First Strand cDNA Synthesis Kit	Thermo Fisher	K1671	
chemical compound, reagent	iTaq Universal SYBR Green Supermix	Invitrogen	1725121	
recombinant DNA reagent	*hrg-9* F	This paper	PCR primers	GGACCCGCTGCCATACACTAATC
recombinant DNA reagent	*hrg-9* R	This paper	PCR primers	GACAATTCAAATCTGGCATCGTG
recombinant DNA reagent	*hrg-10* F	This paper	PCR primers	AGGCTTCCCGGAGCACATTTAC
recombinant DNA reagent	*hrg-10* R	This paper	PCR primers	CAGGCTCCATGCGTCTATCCAG
recombinant DNA reagent	*act* F	This paper	PCR primers	CAACACTGTTCTTTCCGGAG
recombinant DNA reagent	*act* R	This paper	PCR primers	CTTGATCTTCATGGTTGATGGG
gene (Danio rerio)	*tango2*	ENSMBL	ENSDARG00000056550	Zebrafish homolog of TANGO2
strain, strain background (Danio rerio, Sex NA) Sex is not	TUAB	Zebrafish International Resource Center	TU (ZL57) AB (ZL1)	Wild-type lines

determined in Danio Rerio at the age group animals used in this study.				
genetic reagent	*sgRNA to tango2*	Thermofisher Scientific	Kim et al., 2023	Guide RNA to create mutations in tango2 gene
sequence-based reagent	*tango2 F*	Kim et al., 2023	PCR primer	ATGGCTGAAAGAGCTGTGCT
sequence-based reagent	tango2 R	Kim et al., 2023	PCR Primer	ATGGCTGAAAGAGCTGTGCT
chemical compound, drug	Alexa Fluor 488-Phalloidin	Thermofisher Scientific	A12379	1:40 dilution
chemical compound, drug	Methylcellulose	Sigma-Aldrich	M0387-500G	1% w/v dilution
software, algorithm	Prism	Graphpad		
Special Instrumentation	Zebrafish automated activity monitor	Zantiks	ZantiksMWP	
gene (Saccharomyces cerevisiae)	ygr127w	Saccharomycs Genome Database (SGD)	S000003359	Yeast homolog of human Tango2
strain, strain background: S.cerevisiae, haploid, MATa	BY4741(MATa his3Δ1 leu2Δ0 met15Δ0 ura3Δ0)	EUROSCARF		
strain, strain background: S.cerevisiae, haploid, MATα	BY4742 (his3Δ1 leu2Δ0 lys2Δ0 ura3Δ0)	EUROSCARF		
strain, strain background: S.cerevisiae, haploid, MATa	W301(leu2-3,112 trp1-1 can1-100 ura3-1 ade2-1 his3-11,15)	Lab stock		
genetic reagent	YGR127W::KanMX in	Lab stock, Chen Lab,	YGR127W::KanMX	Sun et al., 2022

(S. cerevisiae)	BY4741, BY4742	Zhejiang University		
genetic reagent (include species here) (S. cerevisiae)	YGR127W:: KanMX in W303	This paper	YGR127W::Kan MX	Deletion strain generated by PCR replacement. verified by locus-specific PCR.
genetic reagent	sgRNA: *ygr127w*	Integrated DNA Technologi es (IDT)		Guide RNA sequence used for CRISPR-Cas9–mediated deletion of YGR127W; replaced with KanMX resistance cassette to generate ygr127wΔ strain.
recombinant DNA reagent	pRS313-YGR127W (HIS3, CEN6	This paper		Yeast centromeric plasmid expressing **YGR127W** used forcomplementation
sequence-based reagent	ygr127wgR NA-F	This paper	sgRNA: *ygr127w*	GACTTTAATACGAAATCAAGA TCCCG
sequence-based reagent	ygr127wgR NA-R	This paper	sgRNA: *ygr127w*	AAACCGGGATCTTGATTTCGT ATTAA
sequence-based reagent	ygr127 F	This paper	PCR Primer	AGTCGGATCCTCAAGGTTCTT CTCTAGAACC
sequence-based reagent	ygr127 R	This paper	PCR Primer	AGTCGGATCCTGCTCTATTG GAGAACTTAACC
sequence-based reagent	ygr127 F	This paper	PCR Primer	TTGGCATCTGCCTAGCTTTCG
sequence-based reagent	ygr127 R	This paper	PCR Primer	AGCGTCTACTGTGGTTACTG
commercial assay or kit	Q5 High-Fidelity DNA Polymerase	New England Biolabs (NEB)		Cloning of inserts into pRS313 backbones.
commercial assay or kit	T4 DNA Ligase	New England Biolabs (NEB)		Cloning of inserts into pRS313 backbones.
commercial assay or kit	CutSmart Buffer and Restriction Enzymes	New England Biolabs (NEB)		Cloning of inserts into pRS313 backbones.

	(EcoRI, XhoI, BamHI)			
commercial assay or kit	Golden Gate Assembly Kit (Type IIS cloning)	New England Biolabs (NEB)		Used for one-pot modular assembly of plasmid constructs
commercial assay or kit	EZ Yeast Transformation Kit	Zymo Research	Used for high-efficiency yeast transformation during plasmid integration and complementation assays.	

Worm strains and maintenance: Worm strains used include Bristol N2 (obtained from Caenorhabditis Genetics Center (CGC) at the University of Minnesota), DKO (CCH303 (hrg-9(cck301)V; hrg-10(cck302)V) obtained from C. Chen, and eat-2(ad465), obtained from the Samuelson lab at the University of Rochester. All worms were maintained at 20º C on standard nematode growth medium (NGM) plates with OP50 *E. coli.* All *C. elegans* assays were performed and scored by blinded observers.

GaPP survival assay: Standard OP50 NGM plates treated with 1, 2, 5, or 10 µM gallium protoporphyrin IX (GaPP; Santa Cruz) after seeding. Plates were swirled to ensure an even distribution of GaPP and allowed to dry completely. Adult worms were placed on plates, permitted to lay eggs for 24 hours, and were then removed. Offspring were assessed 72 hours later for survival and were scored as dead if they did not respond to prodding with a platinum wire worm pick.

Pharyngeal pumping: L4 worms were observed and video recorded for 60 second intervals. The number of pharyngeal pumps per minute was manually counted.

Lawn avoidance: L4 worms were placed in the center of OP50 *E. coli* lawns on standard NGM plates and incubated at 20º C for 24 hours. Plates were examined 24 hours later and the numbers of worms remaining on the lawn or on unseeded agar were counted. Worms found on the sides of the dish or otherwise absent from NGM surface were scored as off the plate.

Brood size: For 24-hour brood assessments, young adult worms were placed on plates and allowed to lay eggs for 24 hours before being removed. Viable offspring were counted 48 hours later. For total brood assessments, L4 worms were placed on plates and moved to fresh plates every 24 hours for 5 days to ensure all eggs were accounted for. Viable offspring from eggs laid on each plate were counted 48 hours later and summed.

ZnMP fluorescence: L4 worms grown on OP50 plates were placed on plates treated with 40 uM zinc mesoporphyrin (ZnMP; Santa Cruz) for 16 hours before being washed in M9 buffer, aenesthetized in sodium axide, and mounted on slides with 2% agarose pads for imaging. Worms in the starved condition were placed on uneeded plates for 16 hours before preparation and mounting as above. For liquid media experiments, three generations of worms were cultured in regular heme (20 uM) axenic media, with the first two generations receiving antibiotic-supplemented media (10 mg/ml tetracycline) and the 3rd generation cultivated without antibiotic. L4 worms from the 3rd generation were placed in media containing 40uM ZnMP for 16 hours before being prepared and mounted for imaging as above. Worms were imaged on Zeiss Axio Imager 2 at 40x magnification, with image settings kept uniform across all images. Fluorescent intensity was measured within the proximal region of the intestine using ImageJ.

RNA-seq cluster and gene ontology analysis: The RNA sequencing (RNA-seq) dataset generated by Sun et al. was analyzed with Empirical Analysis of Gene Expression in R (edgeR)

and the top 500 genes were extracted. Computational cluster analysis was done in RStudio. Gene ontology analysis was performed on significantly enriched genes using WormCat.[28] Source code is available in supplemental materials.

Stress conditions and RT-qPCR: N2 worms were subjected to the following stress conditions prior to RNA extraction: 1) fasting: worms were deprived of OP50 E. coli for 24 hours; 2) heat: worms were incubated for 4 hours at 34º C; 3) paraquat: worms were placed on standard NGM/OP50 plates treated with 25 mM paraquat (methyl viologen dichloride hydrate; Sigma Aldrich) for 24 hours. Whole worm RNA was extracted with TRIzol (Invitrogen) and purified using the RNeasy Mini Kit (Qiagen). cDNA generation was performed with the Maxima First Strand cDNA Synthesis Kit (Thermo Fisher). qPCR was performed in triplicate using iTaq Universal SYBR Green Supermix (Invitrogen) with a CFX Duet Realtime qPCR machine (BioRad). Gene expression was normalized to worm *act* and analyzed using the ΔΔCq method. Primers used were as follows:

hrg-9: GGACCCGCTGCCATACACTAATC and GACAATTCAAATCTGGCATCGTG

hrg-10: AGGCTTCCCGGAGCACATTTAC and CAGGCTCCATGCGTCTATCCAG

act: CAACACTGTTCTTTCCGGAG and CTTGATCTTCATGGTTGATGGG

Yeast strain construction: *YGR127w* was knocked out by homologous recombination. A strain (BY4741) harboring a *ygr127w*D was used as a template and the knockout cassette was amplified by PCR using the following primers that anneal upstream and downstream of the locus: TTGGCATCTGCCTAGCTTTCG and AGCGTCTACTGTGGTTACTG

The PCR amplicon was then transformed into W303-1a cells and transformants were selected on YPD plates containing 200mg/ml G418. Integration at the correct locus was confirmed by PCR using the same primers, as above. To complement the *ygr127w*D in the Sun et al. strain, wild type *YGR127w* was amplified with 400 base pairs on either side of the gene and cloned

into a *HIS3*-containing plasmid (pRS413). Transformants were selected on synthetic complete (SC) medium lacking histidine.

Yeast growth curves: Cells were grown to stationary phase at 25°C in either SC or SC-histidine medium. Cultures in the same medium were inoculated at an OD600 of ~0.01 in a 100ml volume in a 96-well plate. The OD600 was read every 15 minutes on a Sunrise Tecan microplate reader.

Zebrafish: All procedures involving zebrafish were approved by the Brigham and Women's Hospital Animal Care and Use Committee. Fish were bred and maintained using standard methods as described.[29] tango2bwh210 and tango2bwh211 zebrafish lines were created in our laboratory by the CRISPR-Cas9 approach as described previously.[22] The tango2bwg210 allele has an insertion of seven bases (c.226_227ins7; p.Tyr76Leufs*25) and tango2bwg211 has a 26 base insertions in exon2 (c.226_227ins26; p.Tyr76Leufs*207) resulting in frameshift mutations and loss of protein function. Whole mount phalloidin staining and microscopy was performed as described previously.[30]

Statistics and Reproducibility: All statistical analyses were performed in GraphPad Prism 9. Data presented are mean ± S.E.M. One-way analysis of variance (ANOVA) followed by Bonferroni's multiple comparisons was used to determine statistical significance ($p < 0.05$). Sample sizes were not pre-determined.

Contributions:

SJM, SES, KSY, APW, and LW designed the *C. elegans* experiments. SES, KSY, OG, and MBB performed the *C. elegans* experiments and analyzed the data. LDO performed the RNA-

seq analysis. MS designed the yeast experiments. AN performed the yeast experiments and analyzed the data. VAG and ESK designed the zebrafish experiments, and EK performed these experiments. VAG and ESK analyzed the zebrafish data. SJM and SES wrote the initial draft of the manuscript. All authors reviewed the manuscript and contributed to its final version.

Acknowledgements:

The authors would like to thank Dr. Keith Nehrke and Dr. Paul Brookes for their guidance and manuscript review, the Chen lab for providing the *hrg-9*/*hrg-10* knockout nematode strain, and the Samuelson lab for supplying the *eat-2* nematode strain. SES is a trainee in the Medical Scientist Training Program funded by NIH T32 GM007256. SJM is supported by National Institutes of Health (NIH) National Institute of Neurological Disorders and Stroke Grant #2K12NS098482-06. This work was funded in part by grants from the TANGO2 Research Foundation to VAG, MS, and to SJM and LW.

Competing Interests:

The authors declare the following competing interests:

The following authors have unpaid roles at the TANGO2 Research Foundation:

SES, Early Diagnostic and Detection Committee Member

VAG, Scientific Advisor Board Member

MS, Scientific Advisory Board Member, Executive Board Member

SJM, Scientific Advisory Board Chair, Executive Board Member

Data Availability Statement:

All raw data from worm behavior, yeast, zebrafish, and RNA-seq studies are available as a supplement to this paper.

References:

1 Kremer, L. S. et al. Bi-allelic Truncating Mutations in TANGO2 Cause Infancy-Onset Recurrent Metabolic Crises with Encephalocardiomyopathy. Am J Hum Genet 98, 358-362 (2016). https://doi.org/10.1016/j.ajhg.2015.12.009

2 Lalani, S. R. et al. Recurrent Muscle Weakness with Rhabdomyolysis, Metabolic Crises, and Cardiac Arrhythmia Due to Bi-allelic TANGO2 Mutations. Am J Hum Genet 98, 347-357 (2016). https://doi.org/10.1016/j.ajhg.2015.12.008

3 Powell, A. R., Ames, E. G., Knierbein, E. N., Hannibal, M. C. & Mackenzie, S. J. Symptom Prevalence and Genotype-Phenotype Correlations in Patients With TANGO2-Related Metabolic Encephalopathy and Arrhythmias (TRMEA). Pediatr Neurol 119, 34-39 (2021). https://doi.org/10.1016/j.pediatrneurol.2021.02.011

4 Jennions, E. et al. TANGO2 deficiency as a cause of neurodevelopmental delay with indirect effects on mitochondrial energy metabolism. J Inherit Metab Dis 42, 898-908 (2019). https://doi.org/10.1002/jimd.12149

5 Bard, F. et al. Functional genomics reveals genes involved in protein secretion and Golgi organization. Nature 439, 604-607 (2006). https://doi.org/10.1038/nature04377

6 Milev, M. P. et al. The phenotype associated with variants in TANGO2 may be explained by a dual role of the protein in ER-to-Golgi transport and at the mitochondria. J Inherit Metab Dis 44, 426-437 (2021). https://doi.org/10.1002/jimd.12312

7 Lujan, A. L. et al. TANGO2 is an acyl-CoA binding protein. J Cell Biol 224 (2025). https://doi.org/10.1083/jcb.202410001

8 Heiman, P. et al. Mitochondrial dysfunction associated with TANGO2 deficiency. Sci Rep 12, 3045 (2022). https://doi.org/10.1038/s41598-022-07076-9

9 Lujan, A. L. et al. Defects in lipid homeostasis reflect the function of TANGO2 in phospholipid and neutral lipid metabolism. Elife 12 (2023). https://doi.org/10.7554/eLife.85345

10 Mehranfar, M. et al. Lipidomic analysis of human TANGO2-deficient cells suggests a lipid imbalance as a cause of TANGO2 deficiency disease. Biochem Biophys Res Commun 717, 150047 (2024). https://doi.org/10.1016/j.bbrc.2024.150047

11 Asadi, P., Milev, M. P., Saint-Dic, D., Gamberi, C. & Sacher, M. Vitamin B5, a coenzyme A precursor, rescues TANGO2 deficiency disease-associated defects in Drosophila and human cells. J Inherit Metab Dis (2022). https://doi.org/10.1002/jimd.12579

12 Miyake, C. Y. et al. Natural History of TANGO2 Deficiency Disorder: Baseline Assessment of 73 Patients. Genet Med (2022). https://doi.org/10.1016/j.gim.2022.11.020

13 Sun, F. et al. HRG-9 homologues regulate haem trafficking from haem-enriched compartments. Nature 610, 768-774 (2022). https://doi.org/10.1038/s41586-022-05347-z

14 Han, S., Guo, K., Wang, W., Tao, Y. J. & Gao, H. Bacterial TANGO2 homologs are heme-trafficking proteins that facilitate biosynthesis of cytochromes c. mBio 14, e0132023 (2023). https://doi.org/10.1128/mbio.01320-23

15 Jayaram, D. T. et al. Heme allocation in eukaryotic cells relies on mitochondrial heme export through FLVCR1b to cytosolic GAPDH. Nat Commun (2025). https://doi.org/10.1038/s41467-025-62819-2

16 Lakowski, B. & Hekimi, S. The genetics of caloric restriction in Caenorhabditis elegans. Proc Natl Acad Sci U S A 95, 13091-13096 (1998). https://doi.org/10.1073/pnas.95.22.13091

17 Greer, E. L. & Brunet, A. Different dietary restriction regimens extend lifespan by both independent and overlapping genetic pathways in C. elegans. Aging Cell 8, 113-127 (2009). https://doi.org/10.1111/j.1474-9726.2009.00459.x

18 Van Raamsdonk, J. M. et al. Decreased energy metabolism extends life span in Caenorhabditis elegans without reducing oxidative damage. Genetics 185, 559-571 (2010). https://doi.org/10.1534/genetics.110.115378

19 Byrne, J. J. et al. Disruption of mitochondrial dynamics affects behaviour and lifespan in Caenorhabditis elegans. Cell Mol Life Sci 76, 1967-1985 (2019). https://doi.org/10.1007/s00018-019-03024-5

20 Ghosh, R. & Emmons, S. W. Episodic swimming behavior in the nematode C. elegans. J Exp Biol 211, 3703-3711 (2008). https://doi.org/10.1242/jeb.023606

21 Dimitrov, L. N., Brem, R. B., Kruglyak, L. & Gottschling, D. E. Polymorphisms in multiple genes contribute to the spontaneous mitochondrial genome instability of Saccharomyces cerevisiae S288C strains. Genetics 183, 365-383 (2009). https://doi.org/10.1534/genetics.109.104497

22 Kim, E. S. et al. Intrinsic and extrinsic regulation of rhabdomyolysis susceptibility by Tango2. Dis Model Mech 16 (2023). https://doi.org/10.1242/dmm.050092

23 Yuan, X., Protchenki, O., Philpott, C. C., & Hamza, I. Topologically Conserved Residues Direct Heme Transport in HRG-1-related Proteins. J Biol Chem 287, 4914-4924 (2011). https://doi.org/10.1074/jbc.M111.326785

24 Chen, C., et al. An intercellular heme trafficking protein delivers maternal heme to the embryo during development in C. elegans. Cell 145, 720-732 (2011) https://doi.org/10.1016/j.cell.2011.04.025

25 Homan, R. A., Jadhav, A. M., Conway, L. P. & Parker, C. G. A Chemical Proteomic Map of Heme-Protein Interactions. J Am Chem Soc 144, 15013-15019 (2022). https://doi.org/10.1021/jacs.2c06104

26 Soo, S. K. & Van Raamsdonk, J. M. High confidence ATFS-1 target genes for quantifying activation of the mitochondrial unfolded protein response. MicroPubl Biol 2021 (2021). https://doi.org/10.17912/micropub.biology.000484

27 Di Pede, A. et al. Mild activation of the mitochondrial unfolded protein response increases lifespan without increasing resistance to stress. Open Biol 15, 240358 (2025). https://doi.org/10.1098/rsob.240358

28 Holdorf, A. D. et al. WormCat: An Online Tool for Annotation and Visualization of Caenorhabditis elegans Genome-Scale Data. Genetics 214, 279-294 (2020). https://doi.org/10.1534/genetics.119.302919

29 Westerfield, M. The Zebrafish Book: A Guide for the Laboratory Use of Zebrafish (Danio Rerio). (Institute of Neuroscience. University of Oregon, 2000).

30 Casey, J. G. et al. NRAP reduction rescues sarcomere defects in nebulin-related nemaline myopathy. Hum Mol Genet 32, 1711-1721 (2023). https://doi.org/10.1093/hmg/ddad011

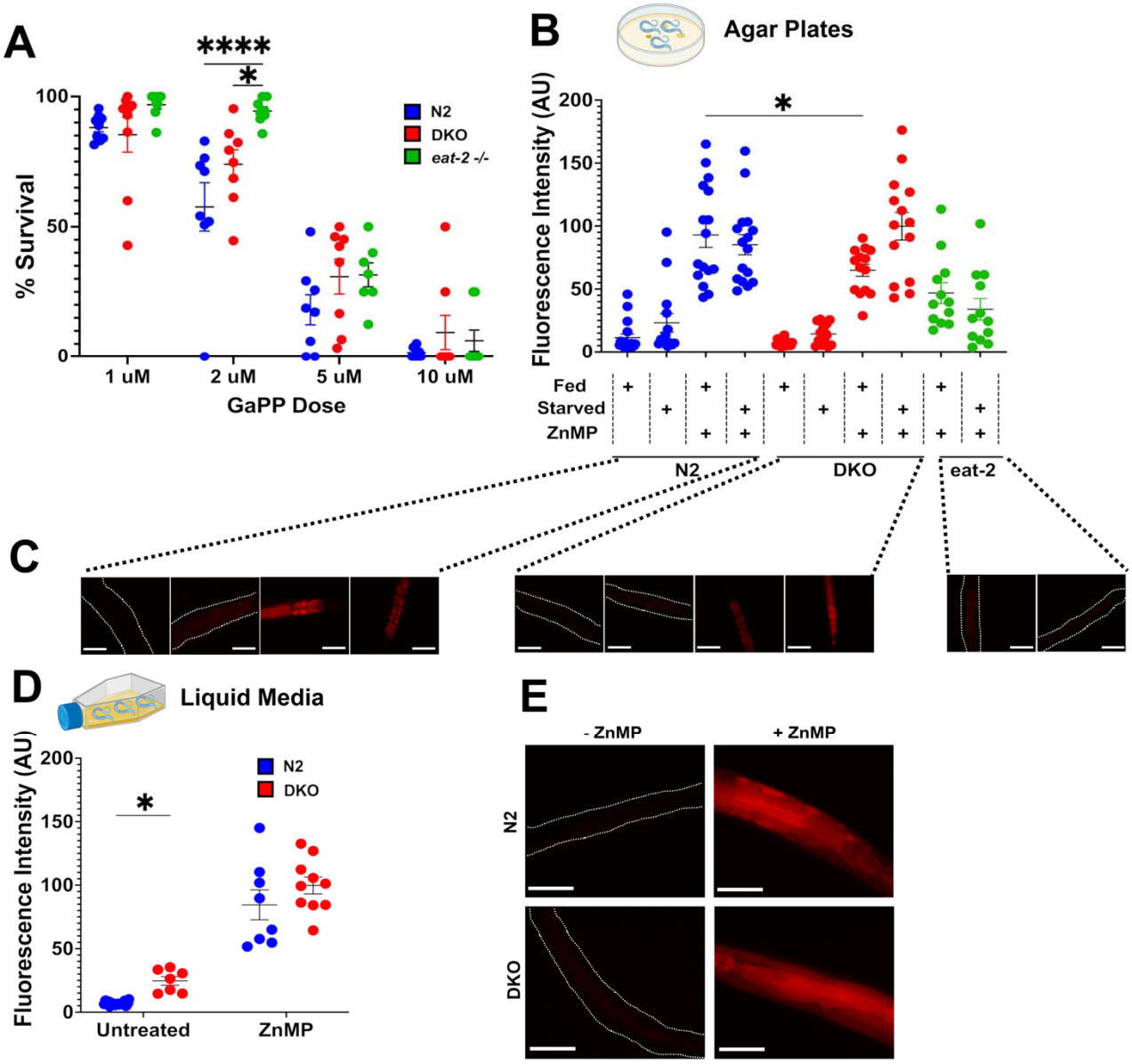

Figure 1: Reduced ingestion of toxic and fluorescent heme analogs may explain differences observed between wildtype *C. elegans* and worms lacking HRG-9 and HRG-10 (double knockout; DKO).

A) Survival of N2, DKO, or *eat-2* knockout worms exposed to 1, 2, 5, or 10 µM GaPP for 72 hours. Each dot represents the number of offspring laid by one adult worm on one GaPP-treated plate after 24 hours. N=3 independent experiments. * $p<0.05$, **** $p<0.0001$ **B)** Quantification of fluorescent staining in N2, DKO, and *eat-2* worms grown on OP50 *E. coli*

plates under fed and starved conditions with or without 40 µM ZnMP treatment. A.U. arbitrary units, N=15 worms analyzed over 3 independent experiments. * $p<0.05$. **C)** Representative images of red fluorescence in N2, DKO, and *eat-2* worms grown on OP50 *E. coli* plates. Scale bars represent 50 µM. **D)** Quantification of fluorescent staining in N2 and DKO cultured in normal heme axenic media with or without 40 µM ZnMP treatment. A.U. arbitrary units, N=7-15 worms analyzed over 3 independent experiments. * $p<0.05$. **E)** Representative images of red fluorescence in N2 and DKO worms grown in liquid media. Scale bars represent 50 µM.

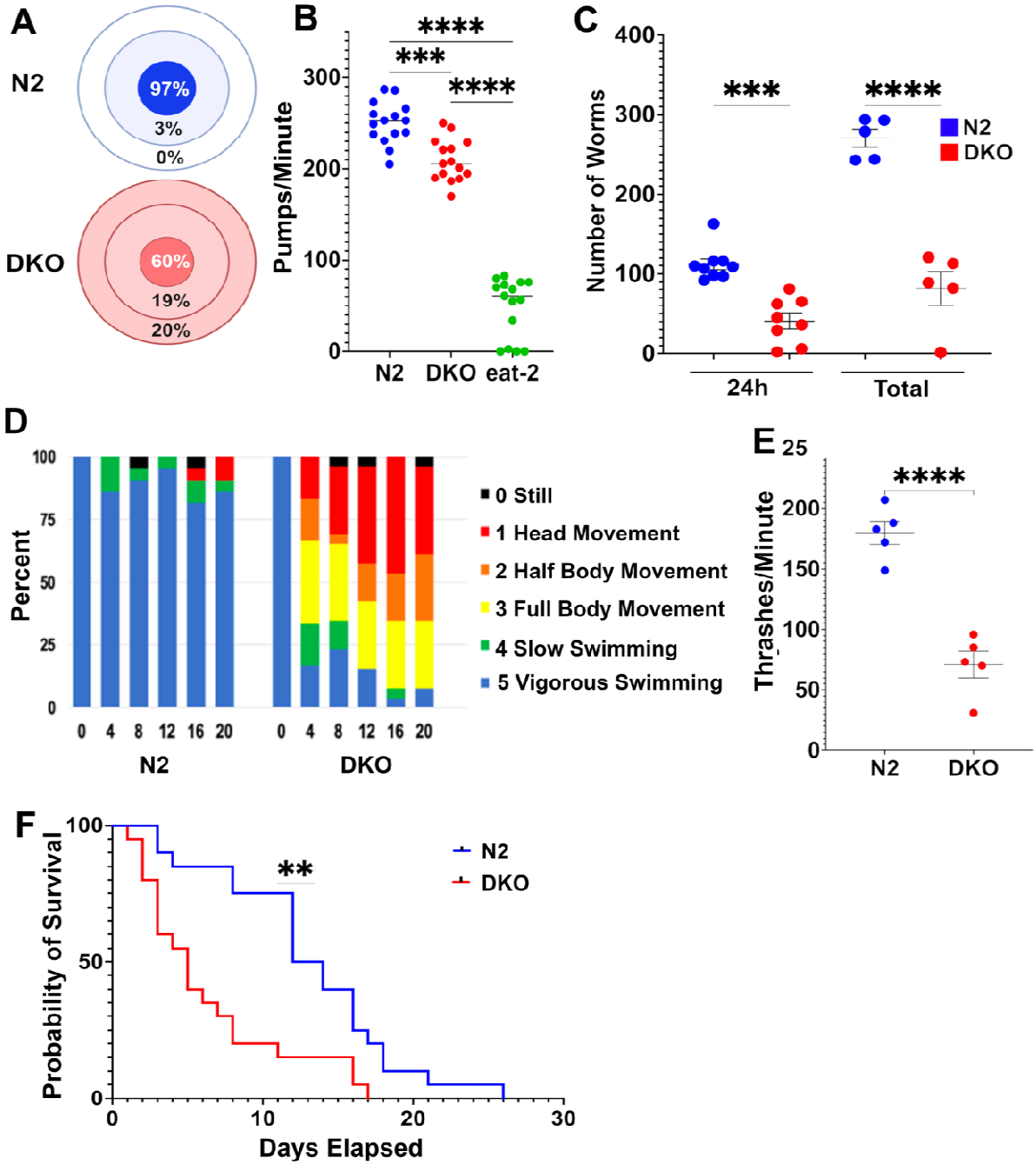

Figure 2: DKO nematodes demonstrate lawn avoidance and reduced pharyngeal pumping, brood sizes, motility, and survival.

A) Proportion of N2 or DKO worms present on OP50 lawn (innermost ring), off OP50 lawn (middle ring), or missing or dead from NGM plate (outer ring). N=180 worms over 3 independent

experiments **B)** Number of of pharyngeal pumps in a one-minute period in N2, DKO, and *eat-2* knockout worms. N=15 worms over 3 independent experiments **C)** Number of viable offspring laid by single adult N2 or DKO worms either after 24 hours of egg lay or across total egg-laying period (5 days). N=8 broods for 24-hour counts, N=5 broods for total brood size counts. **D)** Swimming behavior of N2 and DKO worms over a 20 minute interval**.** Worms were observed at 4 minute intervals and scored from 0-5 on swimming intensity. Bars represent the proportion of worms at each score. **E)** Quantification of thrashes after 4 minutes in M9 buffer. **F)** Longevity of N2 and DKO *C. elegans* observed from L4 larval stage. N=30 worms over 3 independent experiments. (** $p<0.01$, *** $p<0.001$, **** $p<0.0001$).

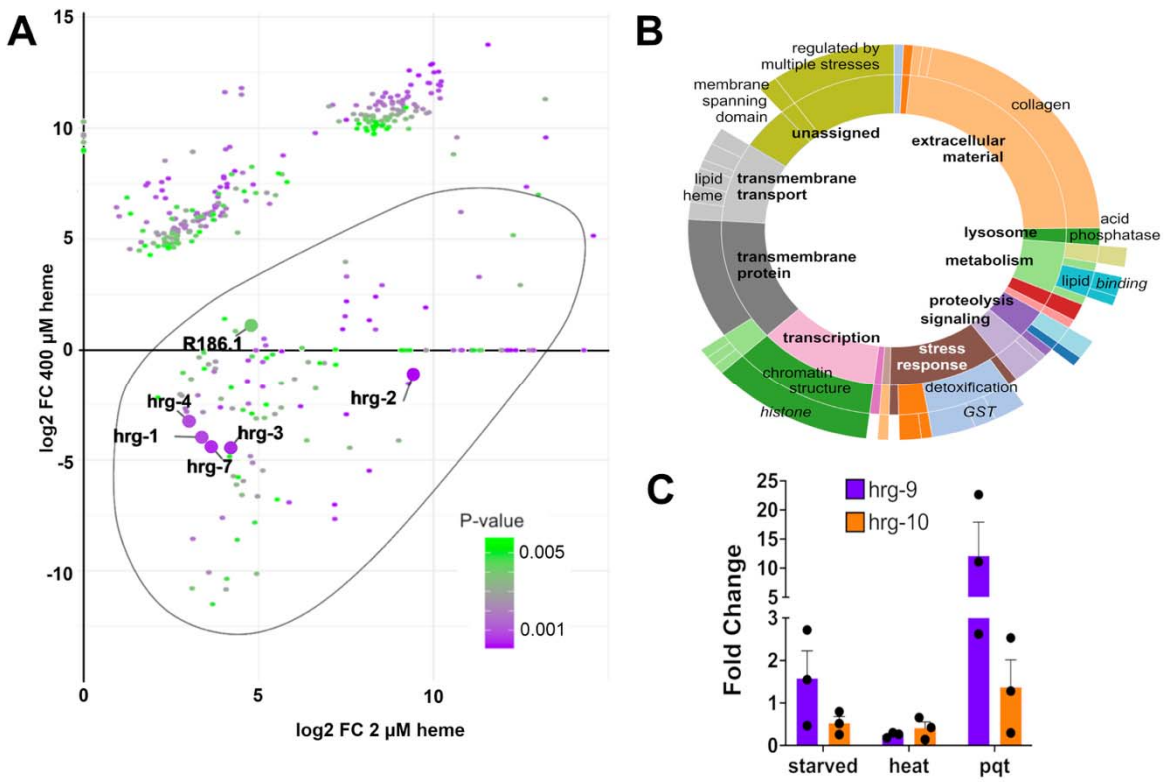

Figure 3: RNA-seq and qPCR analysis show that *hrg-9* and *hrg-10* are not uniquely heme responsive but instead may be preferentially induced under conditions of oxidative stress.

A) Analysis of top 500 genes with differential expression under low heme (2 µM) and high heme (400 µM) conditions. Outline represents 134 relevant genes identified by cluster analysis. R186.1 is the alternative sequence name for *hrg-9*. **B)** Gene ontology analysis identified a variety of biological roles for genes within this cluster **C)** RT-qPCR of *hrg-9* and *hrg-10* under non-heme stress conditions: 24-hour starvation, 4-hour exposure to 34º C heat, and 25 mM paraquat (pqt). N=3 independent experiments.

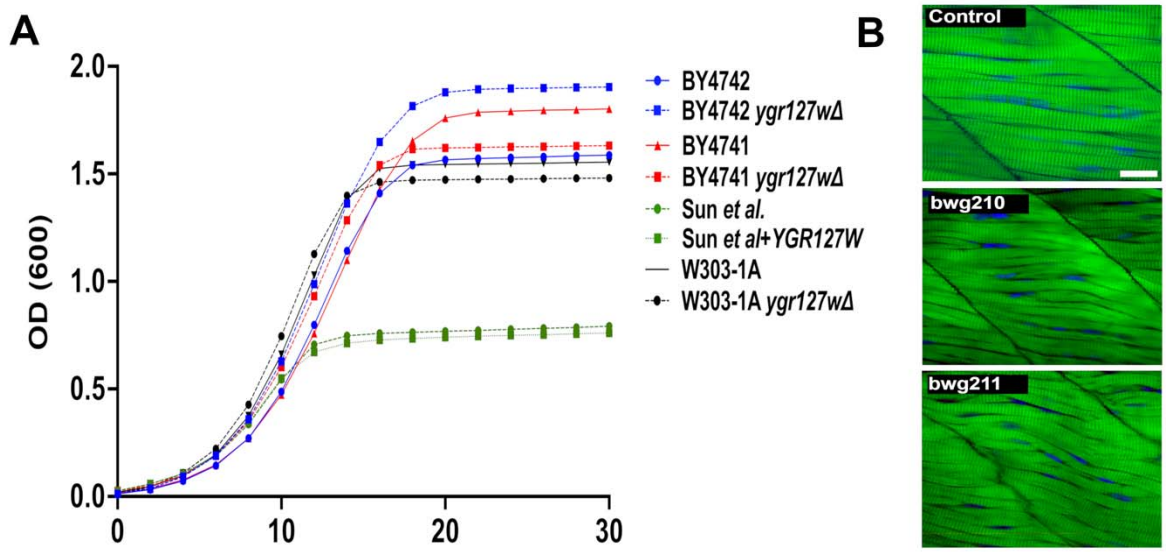

Figure 4: Growth and muscle fiber integrity in yeast and zebrafish models of TANGO2 deficiency fail to replicate previously reported phenotypes.

A) Yeast growth curves. Different strains were grown in SC medium or SC medium lacking histidine at 25º C. **B)** Whole mount phalloidin staining of control and two strains of *tango2*$^{-/-}$ zebrafish (*bwg*^{210} and *bwg*^{211}). Myofibers in mutants lack the parallel organization observed in controls but do not demonstrate significant myofiber breakdown or damage. Representative images; N=8-10 in each group. Scale bar=5 mm.

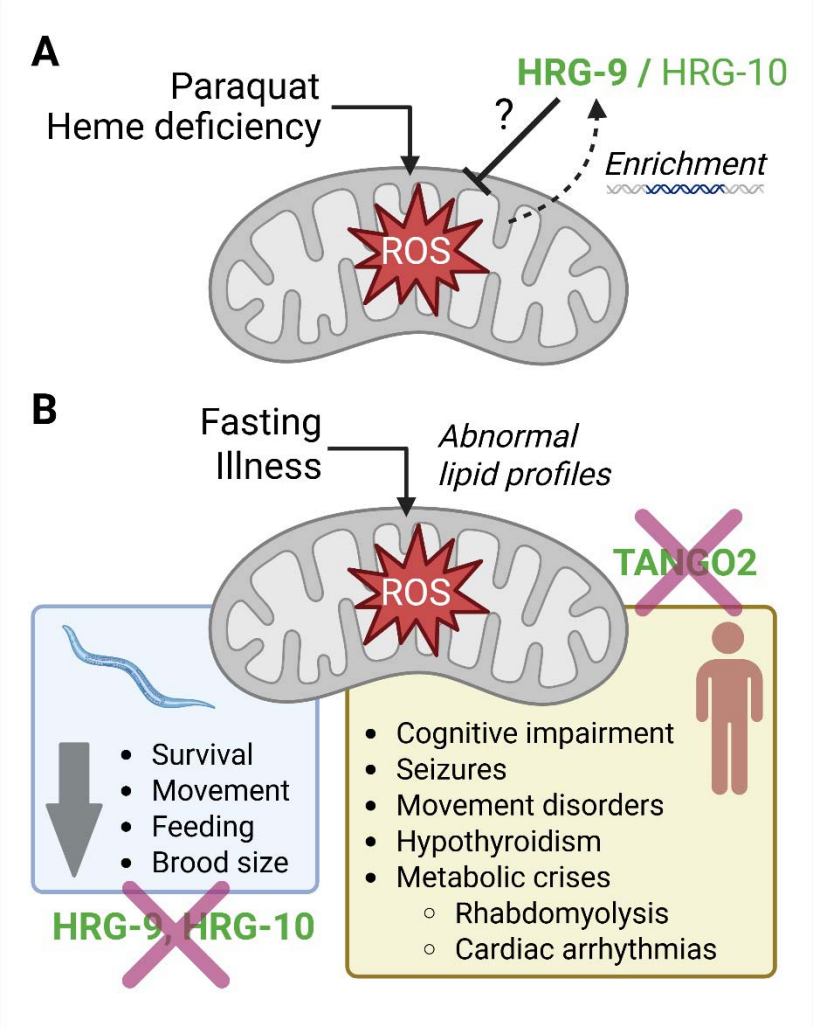

Figure 5: Proposed model of TANGO2 and its homologs acting as stress-responsive mediators of mitochondrial dysfunction.

A) Paraquat exposure and heme deficiency each induce reactive oxygen species (ROS) formation, mitochondrial stress, and enrichment of *hrg-9* in *C. elegans*. TANGO2 and its homologs may help mitigate mitochondrial stress under these conditions, though the exact function of these proteins remains unknown. **B)** Physiological triggers such as fasting or illness also precipitate oxidative stress in the absence of TANGO2. Abnormal lipid profiles have been observed in multiple models of TANGO2 deficiency in the setting of impaired lipid mobilization and reduced fatty acid oxidation. In humans, loss of TANGO2 results in a complex clinical syndrome reminiscent of multiple secondary mitochondrial disorders. In *C. elegans*, loss of hrg-

9 and hrg-10 induces a phenotype previously observed in nematode strains exhibiting mitochondrial dysfunction. Image created with BioRender.

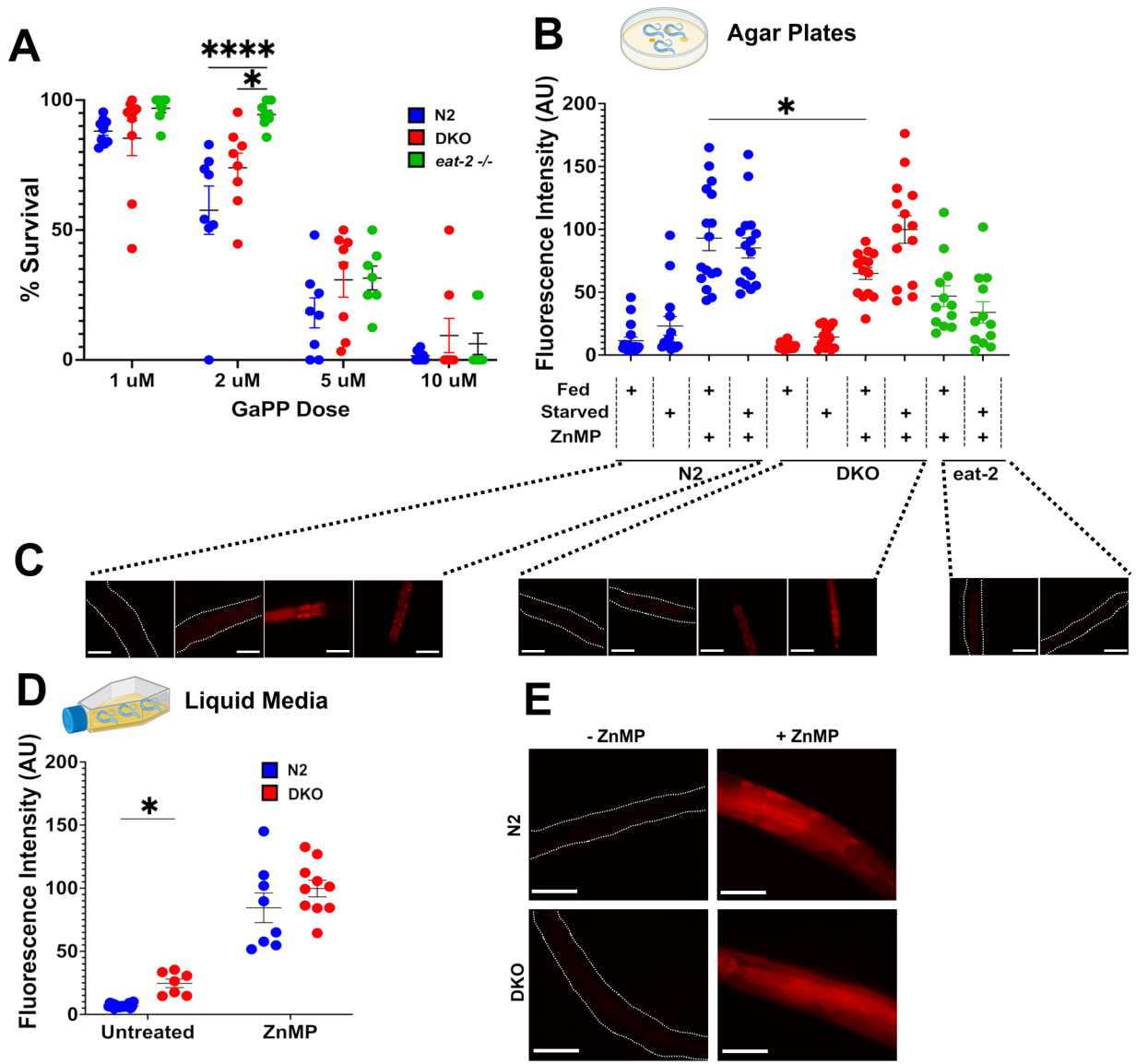
A
****
*
100
50
0
% Survival
N2
DKO
eat-2 -/-
1 uM
2 uM
5 uM
10 uM
GaPP Dose
B
Agar Plates
Fluorescence Intensity (AU)
200
150
100
50
0
*
Fed
Starved
ZnMP
N2
DKO
eat-2
C
D
Liquid Media
Fluorescence Intensity (AU)
200
150
100
50
0
*
N2
DKO
Untreated
ZnMP
E
- ZnMP
+ ZnMP
N2
DKO

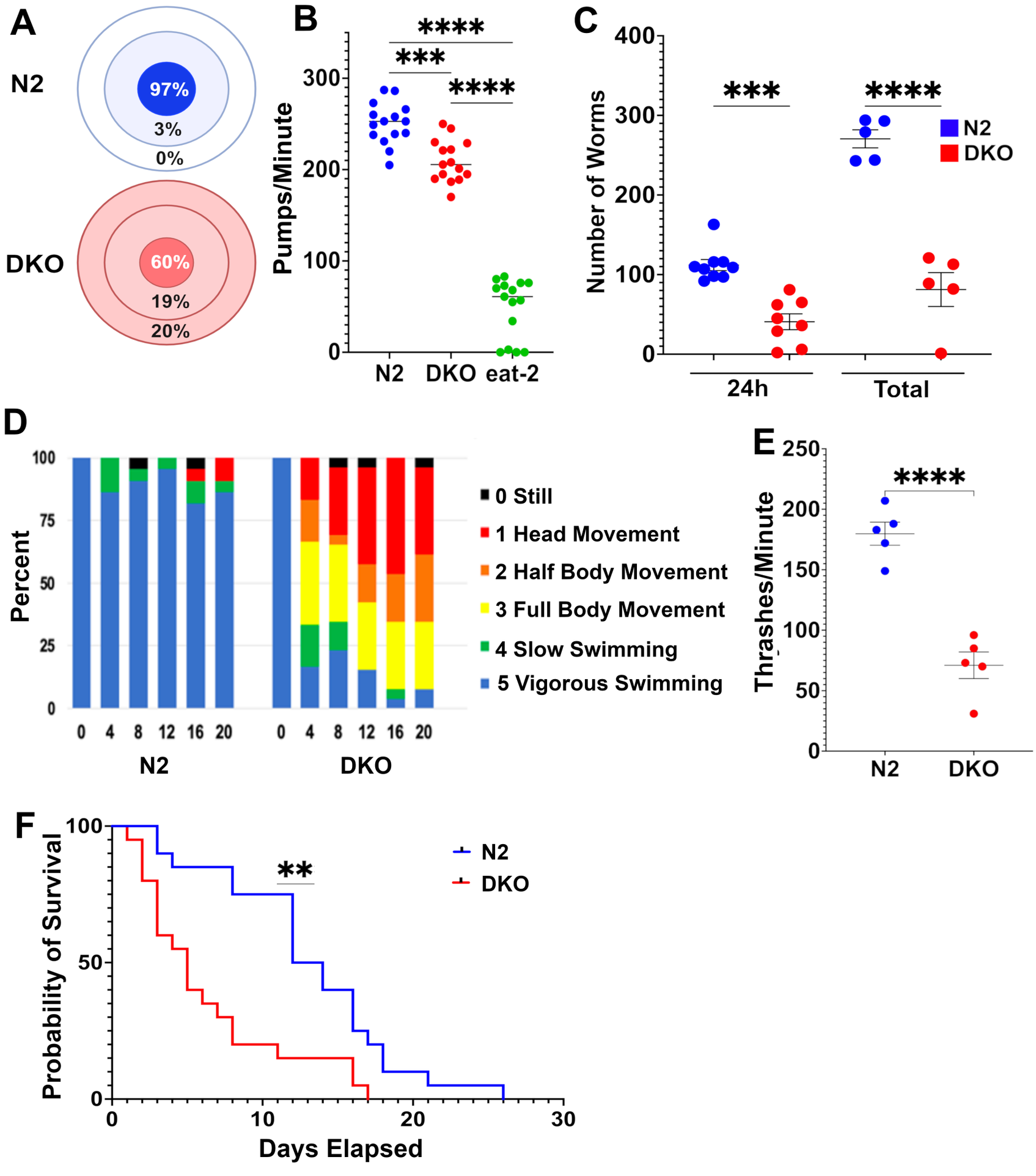
A
N2
97%
3%
0%
DKO
60%
19%
20%
B
Pumps/Minute
****
***
****
N2
DKO
eat-2
C
Number of Worms
***
****
N2
DKO
24h
Total
D
Percent
0 Still
1 Head Movement
2 Half Body Movement
3 Full Body Movement
4 Slow Swimming
5 Vigorous Swimming
N2
DKO
E
Thrashes/Minute
****
N2
DKO
F
Probability of Survival
**
N2
DKO
Days Elapsed

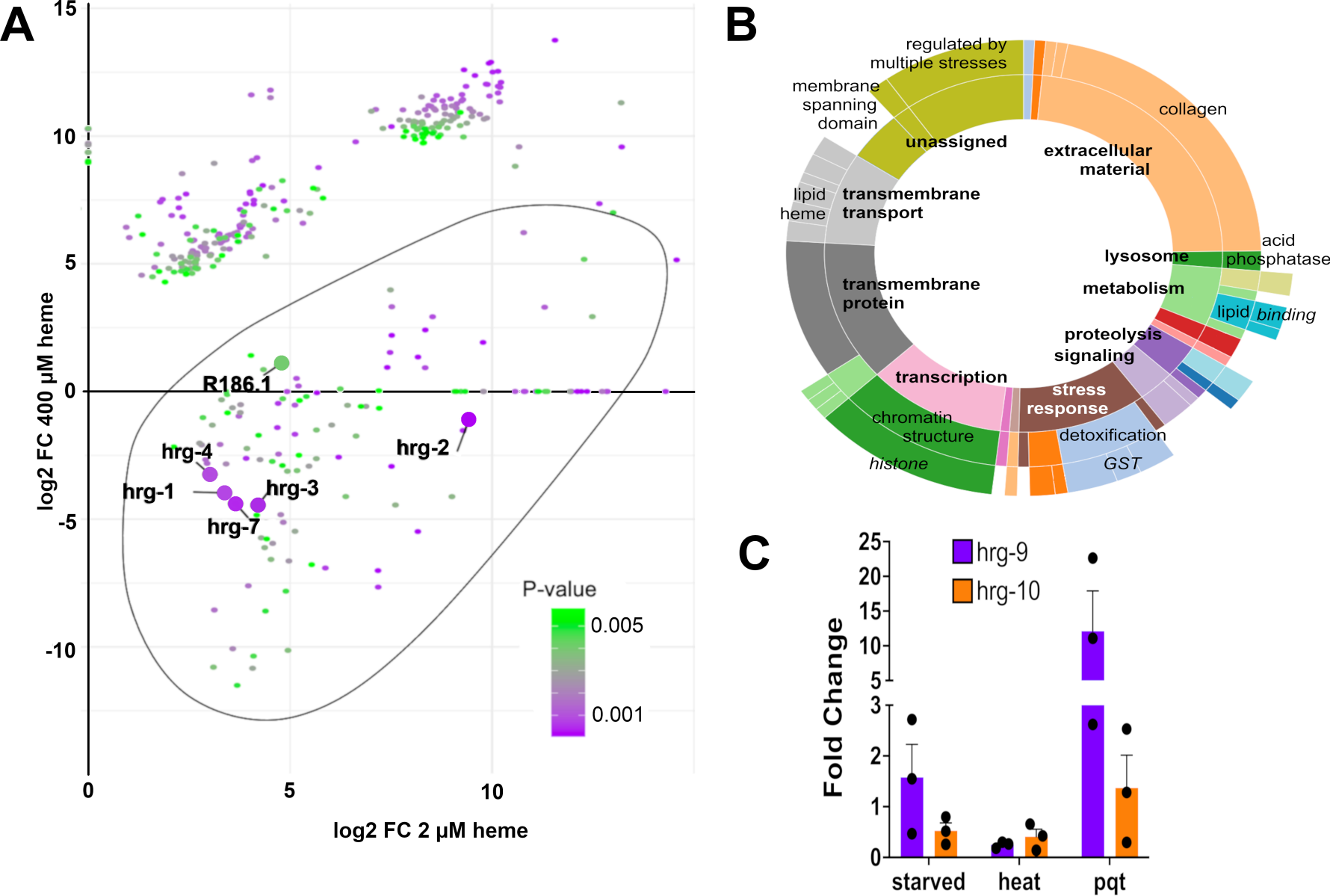
A
log2 FC 400 µM heme
log2 FC 2 µM heme
R186.1
hrg-4
hrg-1
hrg-3
hrg-7
hrg-2
P-value
0.005
0.001
B
regulated by multiple stresses
membrane spanning domain
unassigned
collagen
extracellular material
lipid heme
transmembrane transport
acid phosphatase
lysosome
metabolism
transmembrane protein
lipid binding
proteolysis
signaling
transcription
stress response
chromatin structure
detoxification
histone
GST
C
hrg-9
hrg-10
Fold Change
starved
heat
pqt

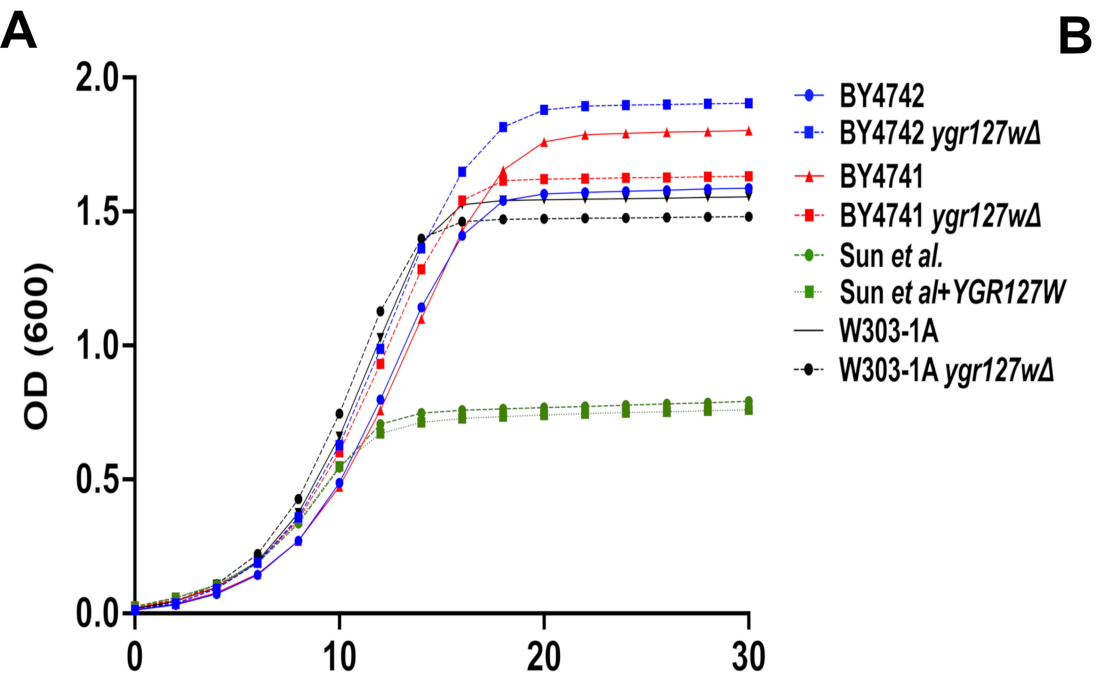
A
OD (600)
2.0
1.5
1.0
0.5
0.0
0
10
20
30
BY4742
BY4742 ygr127wΔ
BY4741
BY4741 ygr127wΔ
Sun et al.
Sun et al+YGR127W
W303-1A
W303-1A ygr127wΔ

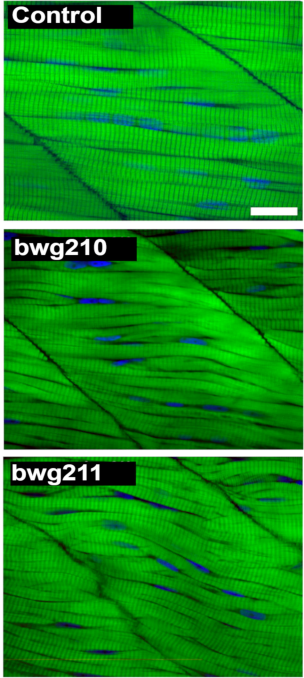
B
Control
bwg210
bwg211

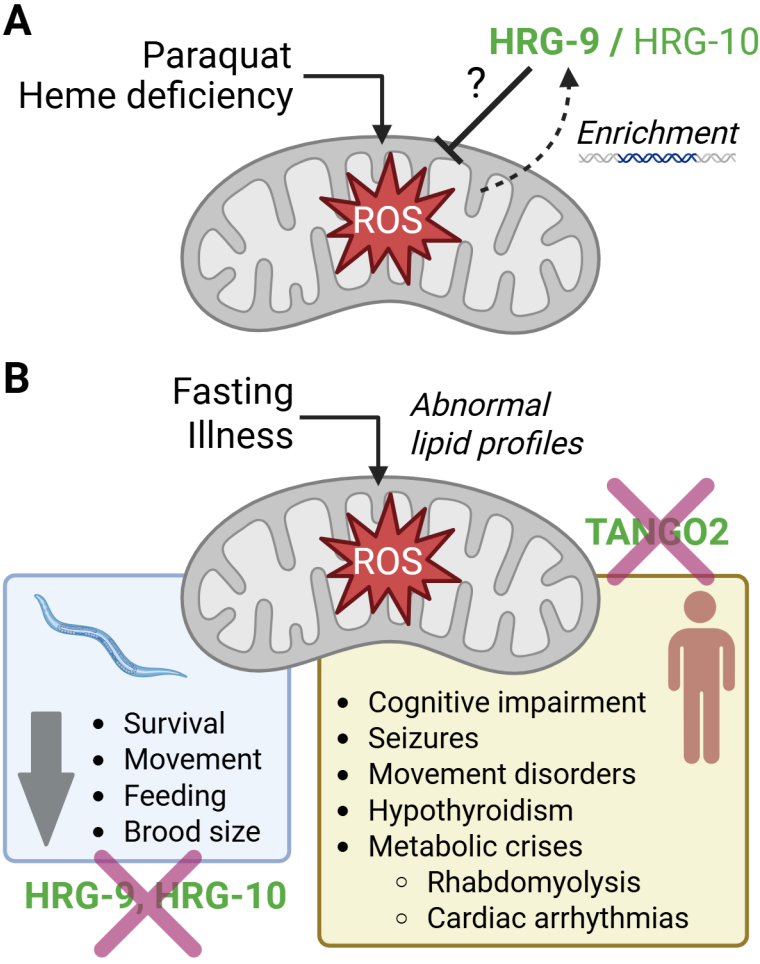
A
Paraquat
Heme deficiency
HRG-9 / HRG-10
?
Enrichment
ROS
B
Fasting
Illness
Abnormal
lipid profiles
ROS
TANGO2
Survival
Movement
Feeding
Brood size
HRG-9, HRG-10
Cognitive impairment
Seizures
Movement disorders
Hypothyroidism
Metabolic crises
Rhabdomyolysis
Cardiac arrhythmias